

# Analysis of the Spin Lattice Model for the Spin-Gapped Layered Compounds $\text{Na}_3\text{Cu}_2\text{SbO}_6$ and $\text{Na}_2\text{Cu}_2\text{TeO}_6$ on the Basis of Electronic Structure Calculations

Hyun-Joo Koo\* and Myung-Hwan Whangbo

Department of Chemistry and Research institute of basic science, Kyung Hee University, Seoul 130-701, Korea, and Department of Chemistry, North Carolina State University, Raleigh, North Carolina 27695-8204

Received June 13, 2007

The spin lattice model for the spin-gapped layered magnetic solids  $\text{Na}_3\text{Cu}_2\text{SbO}_6$  and  $\text{Na}_2\text{Cu}_2\text{TeO}_6$  was examined by evaluating the three spin exchange interactions of their  $\text{Cu}_2\text{MO}_6$  ( $M = \text{Sb}, \text{Te}$ ) layers in terms of spin dimer analysis based on extended Hückel tight binding calculations and mapping analysis based on first principles density functional theory electronic band structure calculations. For both compounds, our calculations show that the two strongest spin exchange interactions, that is, the  $\text{Cu}-\text{O}\cdots\text{O}-\text{Cu}$  super-superexchange ( $J_2$ ) and the  $\text{Cu}-\text{O}-\text{Cu}$  superexchange ( $J_1$ ) interactions, form alternating chains that interact weakly through the  $\text{Cu}-\text{O}-\text{Cu}$  superexchange ( $J_3$ ) interactions. The dominant one of the three spin exchange interactions is  $J_2$ , and it is antiferromagnetic in agreement with the fact that both of the compounds are spin gapped. For  $\text{Na}_3\text{Cu}_2\text{SbO}_6$  and  $\text{Na}_2\text{Cu}_2\text{TeO}_6$ , the superexchange  $J_1$  is calculated to be ferromagnetic, hence, leading to the alternating chain model in which antiferromagnetic and ferromagnetic spin exchange interactions alternate. This picture does not agree with the recent experimental analysis, which showed that the temperature-dependent magnetic susceptibilities of both compounds should be described by the alternating chain model in which two antiferromagnetic spin exchange interactions of different strengths alternate.

## 1. Introduction

The layered magnetic solids  $\text{Na}_3\text{Cu}_2\text{SbO}_6^1$  and  $\text{Na}_2\text{Cu}_2\text{TeO}_6^2$  have a spin gap, namely, they have a spin-singlet magnetic ground state separated from magnetic excited states with an energy gap, thereby leading to zero magnetic susceptibilities below a certain temperature. A spin gap occurs for a magnetic solid typically when the spin lattice of its strong antiferromagnetic spin exchange paths has the pattern of isolated dimers,<sup>3</sup> isolated linear tetramers,<sup>4</sup> isolated

squares,<sup>5</sup> isolated alternating chains,<sup>6</sup> or isolated two-leg ladders.<sup>7</sup> The  $\text{Cu}_2\text{MO}_6$  ( $M = \text{Sb}, \text{Te}$ ) layers of  $\text{Na}_3\text{Cu}_2\text{SbO}_6$  and  $\text{Na}_2\text{Cu}_2\text{TeO}_6$  are made up of edge-sharing  $\text{MO}_6$  and  $\text{CuO}_6$  octahedra (Figure 1).<sup>2,8</sup> Each  $\text{CuO}_6$  octahedron is axially elongated due to its  $\text{Cu}^{2+}$  ion, and the  $\text{CuO}_6$  octahedra are present in the form of edge-sharing  $\text{Cu}_2\text{O}_{10}$  dimers. In the

\* To whom correspondence should be addressed. E-mail: hjkoo@khu.ac.kr (H.-J.K.), mike\_whangbo@ncsu.edu (M.-H.W.).

- (1) Miura, Y.; Hirai, R.; Kobayashi, Y.; Sato, M. *J. Phys. Soc. Jpn.* **2006**, *75*, 84707.
- (2) Xu, J.; Assoud, A.; Soheilnia, N.; Derakhshan, S.; Cuthbert, H. L.; Greedan, J. E.; Whangbo, M. -H.; Kleinke, H. *Inorg. Chem.* **2005**, *44*, 5042.
- (3) (a) Bleaney, B.; Bowers, K. D. *Proc. R. Soc. London* **1952**, *A214*, 451. (b) Kahn, O. *Molecular Magnetism*; VCH Publishers: Weinheim, Germany, 1993.
- (4) (a) Hase, M.; Etheredge, K. M. S.; Hwu, S.-J.; Hirota, K.; and Shirane, G. *Phys. Rev. B* **1997**, *56*, 3231. (b) Belik, A. A.; Azuma, M.; Matsuo, A.; Whangbo, M. H.; Koo, H. J.; Kikuchi, J.; Kaji, T.; Okubo, S.; Ohta, H.; Kindo, K.; Takano, M. *Inorg. Chem.* **2005**, *44*, 6632.

- (5) (a) Taniguchi, S.; Nishikawa, T.; Yasui, Y.; Kobayashi, Y.; Sato, M.; Nishioka, T.; Kotani, M.; Sano, M. *J. Phys. Soc. Jpn.* **1996**, *64*, 2758. (b) Hellberg, C. S.; Pickett, W. E.; Boyer, L. L.; Stokes, H. T.; Mehl, M. J. *J. Phys. Soc. Jpn.* **1999**, *68*, 3489. (c) Korotin, M. A.; Elfimov, I. S.; Anisimov, V. I.; Troyer, M.; Khomskii, D. I. *Phys. Rev. Lett.* **1999**, *83*, 1387. (d) Koo, H.-J.; Whangbo, M.-H. *J. Solid State Chem.* **2000**, *153*, 263.
- (6) (a) Azuma, M.; Saito, T.; Fujishiro, Y.; Hiroi, Z.; Takano, M.; Izumi, F.; Kamiyama, T.; Ikeda, T.; Narumi, Y.; Kindo, K. *Phys. Rev. B* **1999**, *60*, 10145. (b) Koo, H.-J.; Whangbo, M.-H.; VerNooy, P. D.; Torardi, C. C.; Marshall, W. J. *Inorg. Chem.* **2002**, *41*, 4664. (c) Ben Yahia, H.; Gaudin, E.; Darriet, J.; Dai, D.; Whangbo, M. H. *Inorg. Chem.* **2006**, *45*, 5501.
- (7) (a) Azuma, M.; Hiroi, Z.; Takano, M.; Ishida, K.; Kitaoka, Y. *Phys. Rev. Lett.* **1994**, *73*, 3463. (b) Eccleston, R. S.; Uehara, M.; Akimitsu, J.; Eisaki, H.; Motoyama, N.; Uchida, S. I. *Phys. Rev. Lett.* **1998**, *81*, 1702.
- (8) Smirnova, O. A.; Nalbandyan, V. B.; Petrenko, A. A.; Avdeev, M. J. *Solid State Chem.* **2005**, *178*, 1165.

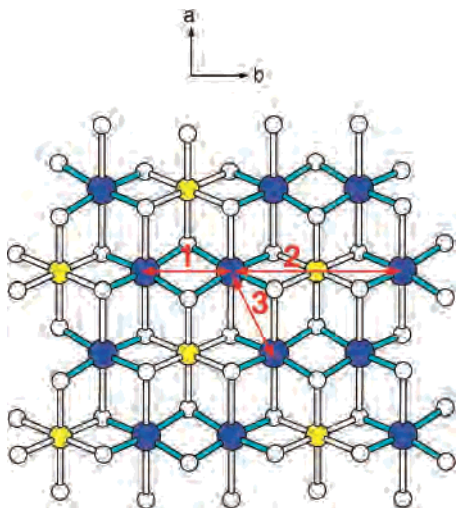


**Figure 1.** Projection view of the  $\text{Cu}_2\text{MO}_6$  layer ( $M = \text{Sb, Te}$ ) found in  $\text{Na}_3\text{Cu}_2\text{SbO}_6$  and  $\text{Na}_2\text{Cu}_2\text{TeO}_6$ . The blue, yellow, and white circles represent the Cu, M, and O atoms, respectively. The numbers 1, 2, and 3 indicate the spin exchange paths  $J_1$ ,  $J_2$ , and  $J_3$ , respectively. The cyan cylinders represent the four shortest Cu–O bonds of each axially elongated  $\text{CuO}_6$  octahedron.

$\text{Cu}_2\text{MO}_6$  ( $M = \text{Sb, Te}$ ) layers, each  $\text{MO}_6$  octahedron is surrounded with four  $\text{Cu}_2\text{O}_{10}$  dimers, and each  $\text{Cu}_2\text{O}_{10}$  dimer with four  $\text{MO}_6$  octahedra, such that the  $\text{Cu}^{2+}$  ions form a honeycomb pattern with the  $M^{n+}$  (i.e.,  $\text{Sb}^{5+}$ ,  $\text{Te}^{6+}$ ) ions occupying the centers of the  $\text{Cu}^{2+}$ -ion hexagons. Because the  $\text{Cu}_2\text{MO}_6$  ( $M = \text{Sb, Te}$ ) layers are well separated by sodium atoms, the magnetic properties of  $\text{Na}_3\text{Cu}_2\text{SbO}_6$  and  $\text{Na}_2\text{Cu}_2\text{TeO}_6$  are described in terms of the spin lattice associated with their  $\text{Cu}_2\text{MO}_6$  ( $M = \text{Sb, Te}$ ) layers. As indicated in Figure 1, there are three spin exchange paths ( $J_1$ ,  $J_2$ , and  $J_3$ ) to consider between the adjacent  $\text{Cu}^{2+}$  ions of a given  $\text{Cu}_2\text{MO}_6$  ( $M = \text{Sb, Te}$ ) layer.  $J_1$  and  $J_3$  are superexchange (SE) interactions involving Cu–O–Cu linkages, whereas  $J_2$  is a super-superexchange (SSE) interaction involving Cu–O••O–Cu linkages.

Miura et al.<sup>1</sup> reported that the magnetic susceptibility of  $\text{Na}_3\text{Cu}_2\text{SbO}_6$  is almost equally well described by three different spin lattice models, that is, an isolated spin dimer model (with  $J/k_B = -139$  K), an alternating chain model with antiferromagnetic–antiferromagnetic (AF–AF) spin exchanges (with  $J/k_B = -143$  K and  $J'/k_B = -38.9$  K), and an alternating chain model with antiferromagnetic–ferromagnetic (AF–F) spin exchanges (with  $J/k_B = -165$  and  $J'/k_B = 209$  K). In describing the spin contribution to the specific heat of  $\text{Na}_3\text{Cu}_2\text{SbO}_6$  below 20 K, however, they reported that the AF–F alternating chain model is better than the isolated dimer and the AF–AF alternating chain models. Xu et al.<sup>2</sup> described the magnetic susceptibility of  $\text{Na}_2\text{Cu}_2\text{TeO}_6$  in terms of an AF–AF alternating chain model (with  $J/k_B = -272$  K and  $J'/k_B = -27$  K), and assigned  $J = J_2$  and  $J' = J_1$  with the help of spin dimer analysis based on extended Hückel tight binding (EHTB) calculations.<sup>9</sup> Miura et al.<sup>1</sup> reported that the magnetic susceptibility of  $\text{Na}_2\text{Cu}_2\text{TeO}_6$

**Table 1.** Geometrical Parameters Associated with the Spin Exchange Paths  $J_1$ ,  $J_2$ , and  $J_3$  of  $\text{Na}_3\text{Cu}_2\text{SbO}_6$  and  $\text{Na}_2\text{Cu}_2\text{TeO}_6$ <sup>a</sup>

path		$\text{Na}_3\text{Cu}_2\text{SbO}_6$	$\text{Na}_2\text{Cu}_2\text{TeO}_6$
$J_1$	Cu•••Cu	2.955	2.858
	$\angle \text{Cu–O–Cu}$	95.3	91.3
$J_3$	Cu•••Cu	3.199	3.214
	$\angle \text{Cu–O–Cu}$	89.6	89.9
$J_2$	Cu•••Cu	5.911	5.817
	O•••O	2.944	2.832
	$\angle \text{Cu–O•••Cu}$	137.2, 137.2	138.9, 138.9

<sup>a</sup> The bond lengths are in units of angstroms, and the bond angles are in units of degrees.

$\text{TeO}_6$  is also well described by isolated dimer and AF–F alternating chain models, obtaining  $J/k_B = -272$  K and  $J'/k_B = 215$  K for the AF–F alternating chain model. By analogy with  $\text{Na}_3\text{Cu}_2\text{SbO}_6$ , Miura et al.<sup>1</sup> suggested that the AF–F alternating chain model should also be correct for  $\text{Na}_2\text{Cu}_2\text{TeO}_6$ . However, the opposite conclusion was reached in the recent study of Derakhshan et al.<sup>10</sup> They analyzed the spin exchange interactions using the EHTB method as well as the  $n$ th-order muffin-tin-orbital (NMTO) downfolding method<sup>11</sup> based on first principles density functional theory (DFT) tight-binding linear muffin-tin-orbital (TB-LMTO) calculations,<sup>12</sup> and showed that the Curie–Weiss temperatures  $\theta$  of the two compounds ( $-55$  and  $-87$  K for  $\text{Na}_3\text{Cu}_2\text{SbO}_6$  and  $\text{Na}_2\text{Cu}_2\text{TeO}_6$ , respectively<sup>2,10</sup>) are much more consistent with the spin exchange parameters deduced from the AF–AF alternating chain model than with those derived from the AF–F alternating chain model.

In the present work, we examine the aforementioned controversy concerning the spin lattice of  $\text{Na}_3\text{Cu}_2\text{SbO}_6$  and  $\text{Na}_2\text{Cu}_2\text{TeO}_6$  by analyzing the spin exchange interactions  $J_1$ ,  $J_2$ , and  $J_3$  of their  $\text{Cu}_2\text{MO}_6$  ( $M = \text{Sb, Te}$ ) layers. For this purpose, we carry out spin dimer analysis based on EHTB calculations as well as mapping analysis based on first principles DFT electronic band structure calculations for a number of ordered spin states of  $\text{Na}_3\text{Cu}_2\text{SbO}_6$  and  $\text{Na}_2\text{Cu}_2\text{TeO}_6$ .

## 2. Qualitative Spin Dimer Analysis

To quantitatively evaluate spin-exchange interactions of a crystalline solid, it is necessary to carry out either first principles electronic structure calculations for the high- and low-spin states of the molecular clusters representing its spin dimers (i.e., structural units containing two adjacent spin sites) or first principles electronic band structure calculations for its ordered spin arrangements.<sup>9a,13–15</sup> A spin exchange

- (10) Derakhshan, S.; Cuthbert, H. L.; Greedan, J. E.; Rahman, B.; Saha-Dasgupta, T. *Phys. Rev. B* **2007**, *76*, 104403.  
 (11) Anderson, O. K.; Saha-Dasgupta, T. *Phys. Rev. B* **2000**, *62*, R16219, and the references cited therein.  
 (12) Anderson, O. K.; Jepsen, O. *Phys. Rev. B* **1984**, *53*, 2571.  
 (13) Noodleman, L. *J. Chem. Phys.* **1981**, *74*, 5737.  
 (14) Illas, F.; Moreira, I.; de, P. R.; de Graaf, C.; Barone, V. *Theor. Chem. Acc.* **2000**, *104*, 265.  
 (15) (a) Chartier, A.; D'Arco, P.; Dovesi, R.; Saunders, V. R. *Phys. Rev. B* **1999**, *60*, 14042, and the references cited therein. (b) Dai, D.; Whangbo, M.-H.; Koo, H.-J.; Rocquefelte, X.; Jobic, S.; Villesuzanne, A. *Inorg. Chem.* **2005**, *44*, 2407.

(9) For reviews see: (a) Whangbo, M.-H.; Koo, H.-J.; Dai, D. *J. Solid State Chem.* **2003**, *176*, 417. (b) Whangbo, M.-H.; Dai, D.; Koo, H.-J. *Solid State Sci.* **2005**, *7*, 827.

**Table 2.**  $(\Delta e)^2$  Values Calculated for the Spin Exchange Paths  $J_1$ ,  $J_2$ , and  $J_3$  of  $\text{Na}_3\text{Cu}_2\text{SbO}_6$  and  $\text{Na}_2\text{Cu}_2\text{TeO}_6^a$ 

path	$\text{Na}_3\text{Cu}_2\text{SbO}_6$	$\text{Na}_2\text{Cu}_2\text{TeO}_6$
$J_1$	260 (0.03)	3300 (0.32) <sup>b</sup>
$J_3$	90 (0.01)	20 (0.00) <sup>b</sup>
$J_2$	5230 (0.51)	10200 (1.00) <sup>b</sup>

<sup>a</sup> The  $(\Delta e)^2$  values are in units of (meV)<sup>2</sup>. The numbers in parentheses are the relative values with respect to the largest  $(\Delta e)^2$  value found for SSE path  $J_2$  of  $\text{Na}_2\text{Cu}_2\text{TeO}_6$ . <sup>b</sup> Taken from ref 2.

parameter  $J$  can be written as  $J = J_F + J_{AF}$ ,<sup>16</sup> where  $J_F$  ( $>0$ ) is the ferromagnetic component, and  $J_{AF}$  ( $<0$ ) is the antiferromagnetic component. In many cases,  $J_F$  is a small positive number and  $J$  is antiferromagnetic (i.e.,  $J < 0$ ), so that the trend in the spin exchange parameters  $J$  of a given compound can be approximated by that in the corresponding antiferromagnetic components  $J_{AF}$ . Of course, there are systems for which  $J$  is ferromagnetic so that the corresponding  $J_F$  term is not negligible.<sup>17</sup> In the spin dimer analysis based on EHTB calculations,  $J_{AF}$  is expressed as<sup>9,16</sup>

$$J_{AF} = -\frac{(\Delta e)^2}{U_{\text{eff}}} \quad (1)$$

where  $\Delta e$  refers to the energy split that results when the two magnetic orbitals of a spin dimer interact, and  $U_{\text{eff}}$  is the effective on-site repulsion, which is essentially constant for a given compound. Consequently, the trend in  $J_{AF}$  is approximated by that in the corresponding  $(\Delta e)^2$  values in the spin dimer analysis based on EHTB calculations. It has been found<sup>9</sup> that the magnetic properties of a variety of magnetic solids are well described by the  $(\Delta e)^2$  values, when both of the d orbitals of the transition metal and s/p orbitals of its surrounding ligands are represented by double- $\zeta$  Slater-type orbitals.<sup>18</sup>

The geometrical parameters associated with the three spin exchange paths  $J_1$ ,  $J_2$ , and  $J_3$  of  $\text{Na}_3\text{Cu}_2\text{SbO}_6$  and  $\text{Na}_2\text{Cu}_2\text{TeO}_6$  are compared in Table 1. The O $\cdots$ O distance of the SSE path  $J_2$  is shorter than the van der Waals distance of 3.08 Å for both compounds and is considerably shorter for  $\text{Na}_2\text{Cu}_2\text{TeO}_6$  than for  $\text{Na}_3\text{Cu}_2\text{SbO}_6$  (2.944 vs 2.832 Å). In addition, the  $\angle\text{Cu}-\text{O}\cdots\text{Cu}$  angles are slightly larger for  $\text{Na}_2\text{Cu}_2\text{TeO}_6$  than for  $\text{Na}_3\text{Cu}_2\text{SbO}_6$ . Therefore, it is expected<sup>9a</sup> that the SSE interaction is substantially antiferromagnetic for both compounds and is more strongly antiferromagnetic for  $\text{Na}_2\text{Cu}_2\text{TeO}_6$  than for  $\text{Na}_3\text{Cu}_2\text{SbO}_6$ .

The  $(\Delta e)^2$  values summarized in Table 2 were calculated using the atomic parameters listed in Table S1 in the Supporting Information.<sup>19</sup> Table 2 shows that, in both  $\text{Na}_2\text{Cu}_2\text{TeO}_6$  and  $\text{Na}_3\text{Cu}_2\text{SbO}_6$ , the SSE interaction  $J_2$  is more strongly antiferromagnetic than the SE interactions  $J_1$  and  $J_3$ . In addition, the spin exchange  $J_2$  is stronger in  $\text{Na}_2\text{Cu}_2\text{TeO}_6$

**Table 3.** Relative Energies (in meV) Per Chemical Unit Cell of the Ordered Spin States AF1, AF2, AF3, and AF4 of  $\text{Na}_3\text{Cu}_2\text{SbO}_6$  and  $\text{Na}_2\text{Cu}_2\text{TeO}_6$  Obtained from Spin-Polarized GGA+U Calculations<sup>a</sup>

	(a) $\text{Na}_3\text{Cu}_2\text{SbO}_6$			
	$U = 4$ eV	$U = 5$ eV	$U = 6$ eV	$U = 7$ eV
AF1	17	16	15	13
AF2	0	0	0	0
AF3	14	13	12	10
AF4	34	28	23	19
	(b) $\text{Na}_2\text{Cu}_2\text{TeO}_6$			
	$U = 4$ eV	$U = 5$ eV	$U = 6$ eV	$U = 7$ eV
AF1	19	18	16	14
AF2	0	0	0	0
AF3	14	13	12	11
AF4	61	51	43	35

<sup>a</sup> The relative energies are given in units of meV with respect to the most stable state AF2.

$\text{TeO}_6$  than in  $\text{Na}_3\text{Cu}_2\text{SbO}_6$  by a factor of 2. The latter prediction is consistent with the antiferromagnetic  $J$  values deduced from the fitting analyses of the magnetic susceptibility data for the two compounds (i.e.,  $-272$  vs  $-165$  K from the AF–F alternating chain model and  $-272$  vs  $-143$  K from the AF–AF alternating chain model).<sup>1,2</sup> Consequently, the antiferromagnetic spin exchange  $J$  deduced from the AF–AF and AF–F alternating chain models should be identified as the SSE interaction  $J_2$ , as reported by Xu et al.<sup>2</sup> and by Derakhshan et al.<sup>10</sup> A shortcoming of the qualitative spin dimer analysis based on EHTB calculations is that it cannot predict whether spin exchange interactions will be ferromagnetic or antiferromagnetic when their  $(\Delta e)^2$  values are small in magnitude (e.g., the SE interactions  $J_1$  and  $J_3$ ). To provide a quantitative prediction for such cases, first principles electronic structure calculations are necessary. This approach is discussed in the next section.

### 3. Quantitative Mapping Analysis of Spin Exchange Interactions

In this section, we evaluate the  $J_1$ ,  $J_2$ , and  $J_3$  parameters of  $\text{Na}_3\text{Cu}_2\text{SbO}_6$  and  $\text{Na}_2\text{Cu}_2\text{TeO}_6$  on the basis of first principles DFT electronic band structure calculations. Our approach is very different from that of Derakhshan et al.,<sup>10</sup> although both rely on first principles DFT electronic structure calculations. In the NMTO downfolding method<sup>11</sup> based on TB-LMTO calculations, the electronic structure of a magnetic insulator is described by the electronic energy bands calculated for its normal metallic state, and the dispersion relations of the resulting partially filled bands are used to extract the hopping integrals needed for discussing the antiferromagnetic contributions  $J_{AF}$  to spin exchange interactions. Therefore, this approach leads to results quite similar to those of the spin dimer analysis based on EHTB calculations.<sup>10</sup> Both approaches are limited in that the ferromagnetic contributions  $J_F$  to spin exchange interactions cannot be evaluated. In the mapping analysis described below, we employ first principles DFT calculations to extract spin exchange parameters that contain both ferromagnetic and antiferromagnetic contributions.

To determine the spin exchange parameters  $J_1$ ,  $J_2$ , and  $J_3$ , we calculate the total energies of several ordered spin states

(16) Hay, P. J.; Thibault, J. C.; Hoffmann, R. *J. Am. Chem. Soc.* **1975**, *97*, 4884.

(17) Hodgson, D. K. *Prog. Inorg. Chem.* **1975**, *19*, 173.

(18) Clementi, E.; Roetti, C. *Atomic Data Nuclear Data Tables* **1974**, *14*, 177.

(19) Our calculations were carried out by employing the CAESAR 2.0 (Crystal and Electronic Structure Analyzer) program package (<http://chvamw.chem.ncsu.edu/>).



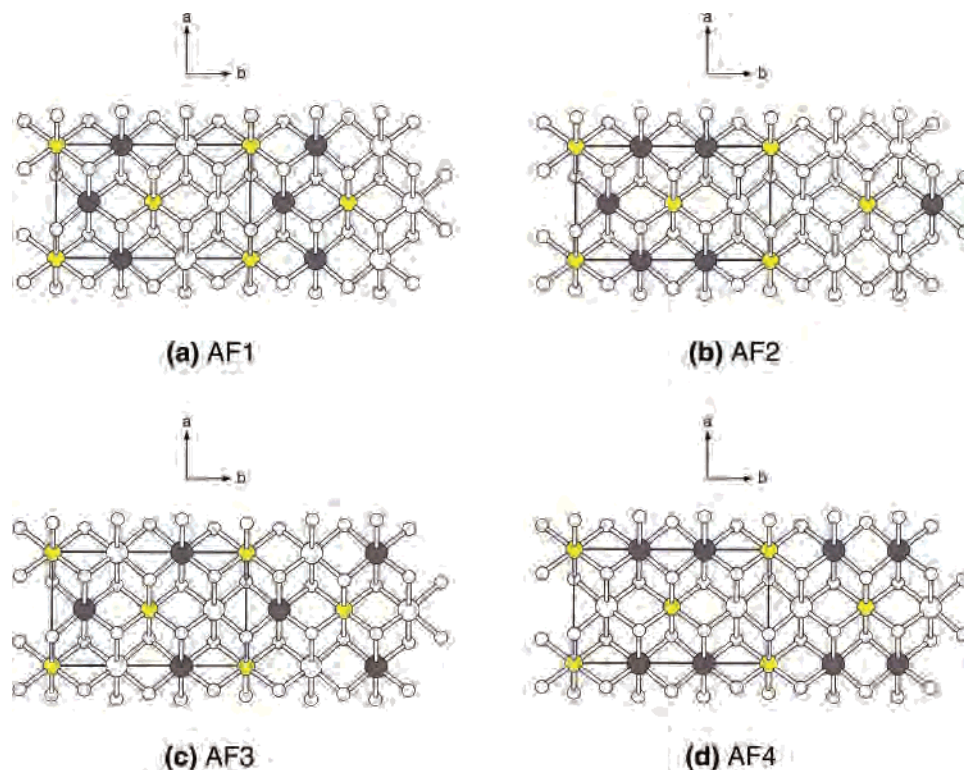


**Figure 2.** Ordered spin arrangements (a) AF1, (b) AF2, (c) AF3, and (d) AF4 in the  $\text{Cu}_2\text{MO}_6$  ( $M = \text{Sb}, \text{Te}$ ) layers of  $\text{Na}_3\text{Cu}_2\text{SbO}_6$  and  $\text{Na}_2\text{Cu}_2\text{TeO}_6$ . The up-spin and down-spins at the copper sites (the largest circles) are represented by the presence and absence of shading, respectively.

of  $\text{Na}_3\text{Cu}_2\text{SbO}_6$  and  $\text{Na}_2\text{Cu}_2\text{TeO}_6$ , and relate the energy differences between these states to the corresponding energy differences expected from the spin Hamiltonian expressed in terms of the spin exchange parameters  $J_1$ ,  $J_2$ , and  $J_3$ . Because there are three parameters to determine, we need to consider at least four different ordered spin states in this mapping analysis. The four ordered spin arrangements employed for our calculations, that is, the AF1, AF2, AF3, and AF4 states are shown in Figure 2. The total energies of these states were calculated by performing spin-polarized DFT electronic band structure calculations with the projected augmented-wave method encoded in the Vienna ab initio simulation package.<sup>20</sup> Our calculations employed the generalized gradient approximation (GGA)<sup>21</sup> for the exchange and correlation correction, the plane wave cut off energy of 500 eV, the on-site repulsion  $U$  on copper to ensure that the AF1, AF2, AF3, and AF4 states of  $\text{Na}_3\text{Cu}_2\text{SbO}_6$  and  $\text{Na}_2\text{Cu}_2\text{TeO}_6$  are magnetic insulating states, and the sampling of the irreducible Brillouin zone with 96 k points. Our GGA+ $U$  calculations were carried out for several values of the onsite repulsion  $U$  (i.e., 4, 5, 6 and 7 eV) to see how the value of  $U$  affects our results. It is noted that hybrid functionals<sup>22</sup> are also used in describing the spin exchange interactions of a magnetic solid.

The relative total energies per chemical unit cell (i.e., per two formula units) calculated for the AF1, AF2, AF3, and AF4 states of  $\text{Na}_3\text{Cu}_2\text{SbO}_6$  and  $\text{Na}_2\text{Cu}_2\text{TeO}_6$  are summarized in Table 3. Our calculations show that the most stable state for both  $\text{Na}_3\text{Cu}_2\text{SbO}_6$  and  $\text{Na}_2\text{Cu}_2\text{TeO}_6$  is the AF2 state in which the spins are ferromagnetically coupled in the paths  $J_1$  and are antiferromagnetically coupled in paths  $J_2$  and  $J_3$ . The total energies of the four ordered spin states increase in the order  $\text{AF2} < \text{AF3} < \text{AF1} < \text{AF4}$ . These two observations remain unchanged as the value of  $U$  varies from 4.0 to 7.0 eV.

To extract the values of the spin exchange parameters  $J_1$ ,  $J_2$ , and  $J_3$  from the above electronic structure calculations, we express the total spin exchange interaction energies of the four ordered spin states in terms of the Ising spin Hamiltonian

$$\hat{H} = - \sum_{i < j} J_{ij} \hat{S}_{iz} \hat{S}_{jz} \quad (2)$$

where  $J_{ij}$  ( $= J_1, J_2$ , or  $J_3$ ) is the spin exchange parameter for the spin exchange interaction between the spin sites  $i$  and  $j$ , whereas  $\hat{S}_{iz}$  and  $\hat{S}_{jz}$  are the  $z$  components of the spin angular momentum operators at the spin sites  $i$  and  $j$ , respectively. Then, by applying the energy expressions obtained for spin dimers with  $N$  unpaired spins per spin site (in the present case  $N = 1$ ),<sup>23</sup> the total spin exchange energies per chemical unit cell of the AF1, AF2, AF3, and AF4 states are written as

(20) (a) Kresse, G.; Hafner, J. *Phys. Rev. B* **1993**, *62*, 558. (b) Kresse, G.; Furthmüller, J. *Comput. Mater. Sci.* **1996**, *6*, 15. (c) Kresse, G.; Furthmüller, J. *Phys. Rev. B* **1996**, *54*, 11169.

(21) Perdew, J. P.; Burke, S.; Ernzerhof, M. *Phys. Rev. Lett.* **1996**, *77*, 3865.

(22) (a) Novák, P.; Kuneš, J.; Chaput, L.; Pickett, W. E. *Phys. Status Solidi B* **2006**, *243*, 563. (b) Ruiz, E.; Llunell, M.; Cano, J.; Rabu, P.; Drillon, M.; Massobrio, C. *J. Phys. Chem. B* **2006**, *110*, 115.

(23) (a) Dai, D.; Whangbo, M.-H. *J. Chem. Phys.* **2001**, *114*, 2887. (b) Dai, D.; Whangbo, M.-H. *J. Chem. Phys.* **2003**, *118*, 29.

$$E_{AF1} = (2J_1 + 2J_2 - 4J_3)N^2/4 \quad (3a)$$

$$E_{AF2} = (-2J_1 + 2J_2)N^2/4 \quad (3b)$$

$$E_{AF3} = (2J_1 + 2J_2 + 4J_3)N^2/4 \quad (3c)$$

$$E_{AF4} = (-2J_1 - 2J_2 + 4J_3)N^2/4 \quad (3d)$$

The above equations lead to

$$J_3 = \left(\frac{1}{N^2}\right)(E_{AF3} - E_{AF1})/2 \quad (4a)$$

$$J_1 = J_3 + \left(\frac{1}{N^2}\right)(E_{AF1} - E_{AF2}) \quad (4b)$$

$$J_2 = J_3 + \left(\frac{1}{N^2}\right)(E_{AF2} - E_{AF4}) \quad (4c)$$

Therefore, we obtain the values of  $J_1$ ,  $J_2$ , and  $J_3$  by replacing the energy differences on the right-hand side of eq 4 with the corresponding energy differences obtained from the DFT electronic structure calculations. The results of this mapping analysis are summarized in Table 4 for  $\text{Na}_3\text{Cu}_2\text{SbO}_6$  and in Table 5 for  $\text{Na}_2\text{Cu}_2\text{TeO}_6$ .

Tables 4 and 5 show that, for all of the values of  $U$  employed, the SE interaction  $J_3$  is antiferromagnetic and is much weaker in strength than are interactions  $J_1$  and  $J_2$ . The SSE interaction  $J_2$  is most strongly antiferromagnetic and is approximately two times stronger for  $\text{Na}_2\text{Cu}_2\text{TeO}_6$  than for  $\text{Na}_3\text{Cu}_2\text{SbO}_6$ . This finding is in good agreement with the result of the qualitative spin dimer analysis. For  $\text{Na}_2\text{Cu}_2\text{TeO}_6$  and  $\text{Na}_3\text{Cu}_2\text{SbO}_6$ , the two strongest spin exchange interactions  $J_2$  and  $J_1$  form alternating chains, in agreement with the fact that their temperature-dependent magnetic susceptibilities are well described by the alternating chain models.<sup>1,10</sup> However, SE interaction  $J_1$  is calculated to be ferromagnetic for  $\text{Na}_2\text{Cu}_2\text{TeO}_6$  and  $\text{Na}_3\text{Cu}_2\text{SbO}_6$ . This latter finding is not consistent with the recent conclusion of Derakhshan et al.<sup>10</sup> that, in reproducing their temperature-dependent magnetic susceptibilities, the AF–AF alternating chain model is correct but the AF–F alternating chain model is not (below). Finally, it is noted that the  $J_2$  values determined from the DFT electronic band structure calculations are greater than the corresponding values obtained from the experimental fitting analyses by a factor of approximately two. It is known that DFT electronic structure calculations generally overestimate the magnitude of spin exchange interactions by a factor of up to 4.<sup>23a,24,25</sup>

The ordered spin states AF1, AF2, AF3, and AF4 are broken-symmetry states.<sup>13</sup> For a simple spin system such as a spin dimer, the mapping analysis can be carried out by employing either a Heisenberg Hamiltonian (i.e.,  $-J\hat{S}_1\hat{S}_2$ ) or an Ising Hamiltonian ( $-J\hat{S}_{1z}\hat{S}_{2z}$ ). It was shown<sup>23b</sup> that both Hamiltonians lead to the same energy expressions for the

**Table 4.** Spin Exchange Parameters (in K) and Curie–Weiss Temperatures  $\theta$  (in K) of  $\text{Na}_3\text{Cu}_2\text{SbO}_6$  Calculated from Spin Polarized GGA+U Calculations and Deduced from Magnetic Susceptibility Measurements<sup>a</sup>

	Calculations with $U$				Fitting Analysis with	
	4.0	5.0	6.0	7.0	AF–F <sup>b</sup>	AF–AF <sup>c</sup>
$J_1/k_B$	179	166	150	132	209	–62
$J_2/k_B$	–372	–345	–285	–232	–165	–160
$J_3/k_B$	–21	–19	–16	–14		
$\theta_{3p}$	–59	–54	–42	–32		
$\theta_{2p}$	–48	–45	–34	–25	11	–56

<sup>a</sup>  $\theta_{3p} = (J_1 + J_2 + 2J_3)/4k_B$ , and  $\theta_{2p} = (J_1 + J_2)/4k_B$ . <sup>b</sup> Taken from ref 1. <sup>c</sup> Taken from ref 10. In describing a spin exchange interaction, we used the convention of  $J$  instead of  $2J$ .

**Table 5.** Spin Exchange Parameters (in K) and Curie–Weiss Temperatures  $\theta$  (in K) of  $\text{Na}_2\text{Cu}_2\text{TeO}_6$  Calculated from Spin Polarized GGA+U Calculations and Deduced from Magnetic Susceptibility Measurements<sup>a</sup>

	Calculations with $U$				Fitting Analysis with	
	4.0	5.0	6.0	7.0	AF–F <sup>b</sup>	AF–AF <sup>c</sup>
$J_1/k_B$	190	175	158	139	215	–28
$J_2/k_B$	–733	–617	–516	–425	–272	–270
$J_3/k_B$	–32	–28	–24	–21		
$\theta_{3p}$	–152	–125	–102	–82		
$\theta_{2p}$	–136	–111	–90	–72	–15	–75

<sup>a</sup>  $\theta_{3p} = (J_1 + J_2 + 2J_3)/4k_B$ , and  $\theta_{2p} = (J_1 + J_2)/4k_B$ . <sup>b</sup> Taken from ref 1. <sup>c</sup> Taken from ref 10. In describing a spin exchange interaction, we used the convention of  $J$  instead of  $2J$ .

broken-symmetry spin state of a general spin dimer. Therefore, as long as broken-symmetry states are employed in the mapping analysis, it is justified to employ an Ising Hamiltonian in extracting spin exchange parameters.

#### 4. Discussion

As already pointed out by Derakhshan et al.,<sup>10</sup> the signs and magnitudes of  $J_1$  and  $J_2$  should be consistent with the Curie–Weiss temperature  $\theta$  derived from high-temperature susceptibility data. The application of mean field theory,<sup>26</sup> which is valid in the paramagnetic limit, shows that

$$\theta = \frac{S(S+1)}{3k_B} \sum_i z_i J_i \quad (5)$$

where the summation runs over all of the nearest neighbors of a given spin site,  $z_i$  is the number of nearest neighbors connected by the spin exchange parameter  $J_i$ , and  $S$  is the spin quantum number of each spin site (i.e.,  $S = 1/2$  in the present case). Therefore,

$$\theta = \frac{J_1 + J_2 + 2J_3}{4k_B} \equiv \theta_{3p} \quad (6a)$$

If we neglect the contribution of the weakest interaction  $J_3$ , the Curie–Weiss temperature can be approximated by

$$\theta \approx \frac{J_1 + J_2}{4k_B} \equiv \theta_{2p} \quad (6b)$$

(24) (a) Dai, D.; Koo, H.-J.; Whangbo, M.-H. *J. Solid State Chem.* **2003**, *175*, 341. (b) Dai, D.; Whangbo, M.-H.; Koo, H.-J.; Rocquefelte, X.; Jobic, S.; Villesuzanne, A. *Inorg. Chem.* **2005**, *44*, 2407.  
(25) Grau-Crespo, R.; de Leeuw, N. H.; Catlow, C. R. *J. Mater. Chem.* **2003**, *13*, 2848.

(26) Smart, J. S. *Effective Field Theory of Magnetism*; Saunders: Philadelphia, 1966.

(In eq 6, the subscripts  $3p$  and  $2p$  refer to the use of three and two spin exchange parameters, respectively). The  $\theta_{3p}$  and  $\theta_{2p}$  values calculated by using the spin exchange parameters obtained from the present DFT calculations and from the fitting analysis of the magnetic susceptibility data are summarized in Tables 4 and 5.

As reported by Derakhshan et al.,<sup>10</sup> the experimental  $\theta$  values of  $\text{Na}_3\text{Cu}_2\text{SbO}_6$  and  $\text{Na}_2\text{Cu}_2\text{TeO}_6$  ( $-55$  and  $-87$  K, respectively) are well reproduced by the  $J_1$  and  $J_2$  values deduced from the AF–AF alternating chain model but are poorly described by those deduced from the AF–F alternating chain model; even the sign of  $\theta$  is incorrectly predicted in the case of  $\text{Na}_3\text{Cu}_2\text{SbO}_6$  (i.e.,  $\theta_{2p} = 11$  K). In contrast to the fitted values of Miura et al. using the AF–F alternating chain model,<sup>1</sup> however, the calculated spin exchange parameters of the present study correctly predict that the Curie–Weiss temperature  $\theta$  should be negative for  $\text{Na}_3\text{Cu}_2\text{SbO}_6$  and  $\text{Na}_2\text{Cu}_2\text{TeO}_6$ . They also predict that  $\theta$  should be greater in magnitude for  $\text{Na}_2\text{Cu}_2\text{TeO}_6$  than for  $\text{Na}_3\text{Cu}_2\text{SbO}_6$  by a factor of approximately 2.5. The latter prediction is in reasonable agreement with the trend in the experimental  $\theta$  values (i.e.,  $-87/-55 \approx 1.6$ ). It should be noticed that the fitted  $J_1$  and  $J_2$  values using the AF–F alternating chain model are comparable in magnitude, whereas our calculations show that  $J_1$  is much weaker in strength than  $J_2$ .

In our calculations, the spin exchange  $J_1$  is ferromagnetic because the spin state AF2 is more stable than the spin states AF1 and AF3 (Figure 2). It is desirable to find an unambiguous experimental test with which to determine whether the magnetic properties of  $\text{Na}_2\text{Cu}_2\text{TeO}_6$  and  $\text{Na}_3\text{Cu}_2\text{SbO}_6$  should be described by the AF–F or the AF–AF alternating chain model. For the AF–F alternating chain model, the repeat vector of the magnetic unit cell along the  $b$  direction (i.e., the direction of the alternating chain) is twice that of the chemical unit cell. For the AF–AF alternating chain model, however, the repeat vector of the magnetic unit cell along the  $b$  direction is identical with that of the chemical unit cell (Figure 2). Consequently, one might consider if neutron diffraction experiments can be used to test which model is correct. However, at a low temperature required to detect

local magnetic moments,  $\text{Na}_2\text{Cu}_2\text{TeO}_6$  and  $\text{Na}_3\text{Cu}_2\text{SbO}_6$  would be in the spin-gapped state in which there is no local magnetic moment to detect. Thus, one may wonder if neutron scattering experiments, which provide information about spin-gap and spin-wave dispersion relations, can be of use in distinguishing between the AF–F and AF–AF alternating chain models.

## 5. Concluding remarks

As for the strongest antiferromagnetic spin exchange  $J_2$  leading to the spin-gapped behavior of  $\text{Na}_3\text{Cu}_2\text{SbO}_6$  and  $\text{Na}_2\text{Cu}_2\text{TeO}_6$ , the spin dimer analysis based on EHTB calculations provides the same prediction as does the quantitative mapping analysis based on DFT electronic band structure calculations. In agreement with experiment, our study shows that the spin lattice of for  $\text{Na}_3\text{Cu}_2\text{SbO}_6$  and  $\text{Na}_2\text{Cu}_2\text{TeO}_6$  is given by the alternating chain model, in which the spin exchange interactions  $J_2$  and  $J_1$  alternate. However, our study predicts that spin exchange  $J_1$  is ferromagnetic. The latter is inconsistent with the recent experimental analysis of Derakhshan et al., who showed that the temperature-dependent magnetic susceptibilities of  $\text{Na}_3\text{Cu}_2\text{SbO}_6$  and  $\text{Na}_2\text{Cu}_2\text{TeO}_6$  should be described by the AF–AF alternating chain model. It is of interest to examine if the spin exchange interaction  $J_2$  becomes antiferromagnetic with more sophisticated electronic structure calculations. It is desirable to find a definitive experimental test with which to determine whether the AF–F or the AF–AF alternating chain model is correct for  $\text{Na}_2\text{Cu}_2\text{TeO}_6$  and  $\text{Na}_3\text{Cu}_2\text{SbO}_6$ .

**Acknowledgment.** The work at NCSU was supported by the Office of Basic Energy Sciences, Division of Materials Sciences, U.S. Department of Energy, under Grant DE-FG02-86ER45259. We thank Dr. S. Derakhshan for making the preprint of ref 10 available to us prior to publication.

**Supporting Information Available:** Table of the atomic orbital parameters employed in the present EHTB calculations. This material is available free of charge via the Internet at <http://pubs.acs.org>.

IC701153Z